AJNR

Computational Modeling of Venous Sinus Stenosis in Idiopathic Intracranial Hypertension

M.R. Levitt, P.M. McGah, K. Moon, F.C. Albuquerque, C.G. McDougall, M.Y.S. Kalani, L.J. Kim and A. Aliseda

Computational Modeling of Venous Sinus Stenosis in Idiopathic Intracranial Hypertension

M.R. Levitt, P.M. McGah, K. Moon , F.C. Albuquerque, C.G. McDougall, M.Y.S. Kalani, L.J. Kim, and A. Aliseda

ABSTRACT

BACKGROUND AND PURPOSE: Idiopathic intracranial hypertension has been associated with dural venous sinus stenosis in some patients, but the hemodynamic environment of the dural venous sinuses has not been quantitatively described. Here, we present the first such computational fluid dynamics model by using patient-specific blood pressure measurements.

MATERIALS AND METHODS: Six patients with idiopathic intracranial hypertension and at least 1 stenosis or atresia at the transverse/ sigmoid sinus junction underwent MR venography followed by cerebral venography and manometry throughout the dural venous sinuses. Patient-specific computational fluid dynamics models were created by using MR venography anatomy, with venous pressure measurements as boundary conditions. Blood flow and wall shear stress were calculated for each patient.

RESULTS: Computational models of the dural venous sinuses were successfully reconstructed in all 6 patients with patient-specific boundary conditions. Three patients demonstrated a pathologic pressure gradient (≥ 8 mm Hg) across 4 dural venous sinus stenoses. Small sample size precludes statistical comparisons, but average overall flow throughout the dural venous sinuses of patients with pathologic pressure gradients was higher than in those without them (1041.00 $\pm$ 506.52 mL/min versus 358.00 $\pm$ 190.95 mL/min). Wall shear stress was also higher across stenoses in patients with pathologic pressure gradients (37.66 $\pm$ 48.39 Pa versus 7.02 $\pm$ 13.60 Pa).

CONCLUSIONS: The hemodynamic environment of the dural venous sinuses can be computationally modeled by using patient-specific anatomy and physiologic measurements in patients with idiopathic intracranial hypertension. There was substantially higher blood flow and wall shear stress in patients with pathologic pressure gradients.

ABBREVIATIONS: CFD = computational fluid dynamics; IIH = idiopathic intracranial hypertension; WSS = wall shear stress

Idiopathic intracranial hypertension (IIH), also known as pseudotumor cerebri or benign intracranial hypertension, has been associated with dural venous sinus stenosis.[1,2] While many patients with IIH have anatomic evidence of venous sinus stenosis,[3] cerebral venography and invasive manometry are often used to differentiate patients with a "pathologic" stenosis, which demonstrates a pressure gradient across the stenosis, from those without

such a gradient, to determine which patients may benefit from endovascular stent placement.[4,5] That some patients with IIH present with this pressure gradient and others do not, despite similar anatomic narrowing of the dural venous sinuses, suggests that the mechanism by which IIH is related to venous sinus stenosis may depend on hemodynamic characteristics of dural venous sinus drainage.[6] However, venous manometry measures only blood pressure rather than blood flow through the complex 3D hemodynamic environment of the dural venous sinuses.

Patient-specific computational fluid dynamics (CFD) modeling of the hemodynamic environment of patients with IIH with and without a physiologic stenosis could improve the understanding of IIH pathophysiology and potentially aid in patient selection for endovascular stent placement. In this study, we constructed CFD models of patients' dural venous sinuses, with simulated blood flow informed by patient-specific pressure measurements obtained during invasive cerebral venography, to accurately model the hemodynamics of IIH in patients with dural venous sinus stenosis.

Table 1: Venography and manometry measurements

| Patient | Side | Blood Pressure (mm Hg) | | | | |
		Superior Sagittal Sinus	Transverse Sinus	Sigmoid Sinus	Pressure Gradient (mm Hg)	% Stenosis[a]
1	Left	7	5	2	3	60.34
	Right		7	8	−1	2.41
2	Right	10	8	7	1	2.13
3	Right	23	24	19	5	14.81
4	Left	56	34	16	18	50
	Right		16	15	1	33.33
5	Left	39	29	18	11	82.35
	Right		34	17	17	26.47
6	Right	83	88	7	81	61.64

[a] Defined as the percentage change between the narrowest point of the transverse sinus and the midpoint of the ipsilateral sigmoid sinus.

MATERIALS AND METHODS

Patient Population and Venogram Procedure

Institutional review board approval (Barrow Neurological Institute, Phoenix, Arizona) was obtained for this retrospective study. Six patients with a previous diagnosis of untreated IIH (determined by intracranial pressure of ≥25 cm H_2O without structural or CSF abnormality[7]) and MR venography demonstrating dural venous sinus atresia or stenosis of >50% in at least 1 location underwent cerebral venography with manometry. Cerebral venography was performed with the patient under local anesthesia by using a transfemoral access. A 5F guide catheter (Envoy; Codman & Shurtleff, Raynham, Massachusetts) was navigated into the right jugular bulb, and a microcatheter (Excelsior SL-10; Stryker, Kalamazoo, Michigan) was placed in the dural venous sinuses. Manometry was then performed in the bilateral transverse and sigmoid sinuses and the posterior third of the superior sagittal sinus by transducing the blood pressure through the microcatheter. In 2 patients in whom the transverse and sigmoid sinuses were atretic or absent on 1 side, measurements were obtained in all other locations. Stenoses were considered pathologic if a pressure gradient of ≥8 mm Hg was observed across the segment of narrowed lumen.[5] Patients were grouped into pathologic and nonpathologic groups based on the presence of such a gradient across ≥1 stenotic venous sinus.

Computational Modeling

3D reconstructions of each patient's venous sinuses were created from the preprocedural MR venography by using the Vascular Modeling Toolkit (VMTK; www.vmtk.org), which uses a gradient-based level set method. The model inflows were truncated at the posterior third of the superior sagittal sinus and the midpoint of the straight sinus. The model outflows were truncated at the bilateral distal sigmoid sinuses, unless 1 side was atretic, in which case it was excluded.

Two models were created for each patient: one with a virtual microcatheter in the center of the lumen from the sigmoid sinus through the transverse sinus on the right side (as it was placed during the actual venogram procedure) and one without. We created both models for each patient to address a common concern with venographic manometry, which is that the placement of a microcatheter through a venous sinus stenosis could, in itself, alter the hemodynamics of the venous sinus stenosis and affect the results. The virtual microcatheter was modeled after the Excelsior SL-10 microcatheter used during venographic manometry, with an identical diameter of 0.57 mm.

A computational mesh was also created with VMTK. The spatial resolution of the mesh was a uniform 0.4 mm in all meshes without virtual microcatheter placement, while meshes with the virtual microcatheters decreased in resolution to 0.07 mm around the catheter surface. Meshes had 1–4 million finite volumes. Steady flow CFD simulations were conducted by using Fluent 14 (ANSYS, Canonsburg, Pennsylvania) with a spatially second-order upwind scheme. Blood pressure at the inflow (posterior third of the superior sagittal sinus) and outflow (sigmoid sinuses) as measured by venographic manometry was directly prescribed as the CFD boundary conditions. Gravity was also included in the simulations because pressure measurements in the venous system can be influenced by hydrostatic pressure gradients. The CFD simulations assumed rigid sinus walls and Newtonian blood rheology with a density of 1.05 g/cm³ and a viscosity of 3.5 cP. Flow was determined to be laminar or turbulent on the basis of the results of the CFD calculations, which resolved velocity and pressure fluctuations if present. Laminar flow was not presupposed.

Each patient-specific CFD model was analyzed for blood pressure, flow rate, and wall shear stress (WSS) both with and without the virtual microcatheter. Values of each variable at key anatomic locations (superior sagittal, straight, and sigmoid sinuses) were calculated with and without virtual microcatheter placement, and contour maps of blood pressure and WSS throughout the venous sinuses were created for each patient.

Separate 2D blood flow velocity profiles across dural venous sinus stenoses were created by using the patient-specific flow data. The magnitude of the flow velocity across each stenosis was visualized by manually placing a 2D plane along a longitudinal section of the affected dural sinus.

RESULTS

Sinus measurements and venographic pressures for each patient are shown in Table 1. Three patients had pathologic pressure gradients of ≥8 mm Hg across 4 stenoses (the pathologic group), while 3 other patients did not have a substantial pressure gradient (the nonpathologic group). One patient in the pathologic group and 2 patients in the nonpathologic group had atretic sinus systems on one side. The average severity of the stenosis was 50.76% ± 22.42% in the pathologic group and 24.34% ± 32.31% in the nonpathologic group as determined by the 3D imaging.

Results from CFD simulations are shown in Table 2 and Figs 1 and 2. Data in Table 2 and all figures are displayed on the basis of calculations with the virtual microcatheter in place, to better represent the hemodynamic environment during venous pressure measurements obtained with the microcatheter in vivo. The average outflow was 1041.00 ± 506.52 mL/min for the pathologic group and 358.00 ± 190.95 mL/min for the nonpathologic group.

Table 2: CFD calculations of blood flow and WSS with virtual microcatheter placement

Patient	Side	Blood Flow (mL/min)			Wall Shear Stress (Pa)				WSS Gradient across Stenosis
		Superior Sagittal Sinus	Straight Sinus	Sigmoid Sinus	Superior Sagittal Sinus	Straight Sinus	Transverse Sinus	Sigmoid Sinus	
1	Left	370	50	171	0.72	0.27	29	1.59	27.41
	Right			248			0.36	0.82	−0.46
2	Right	433	78	511	2.59	0.89	1.88	1.16	0.72
3	Right	71	72	144	0.67	0.84	1.33	0.93	0.4
4	Left[a]	1582	0	196	14.74	0.09	8.24	1.21	7.03
	Right			1386			37.94	18.72	19.22
5	Left[a]	457	121	112	2.37	0.82	38.21	4.63	33.58
	Right[a]			466			16.36	9.82	6.54
6	Right[a]	816	147	963	5.23	1.79	163.01	41.07	121.94

[a] Pathologic pressure gradient (≥ 8 mm Hg) on venographic manometry.

Non-pathologic pressure gradient
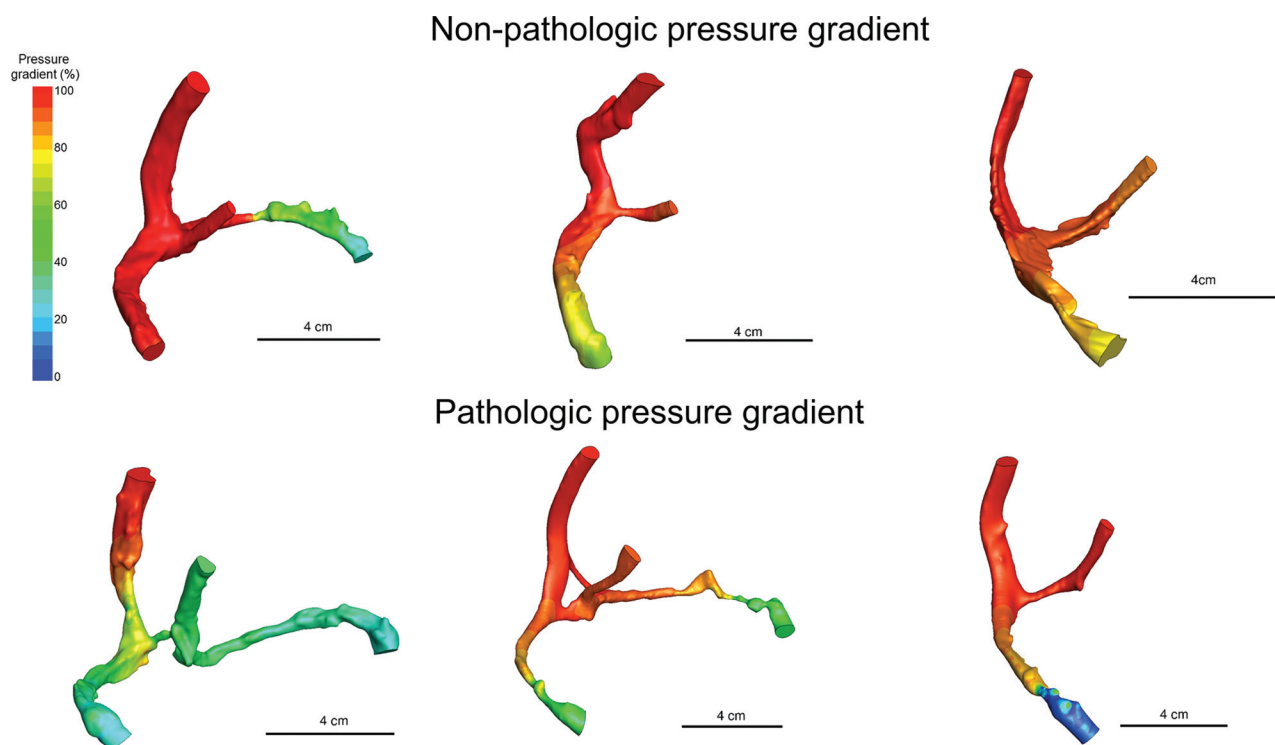

Pathologic pressure gradient

FIG 1. Computational fluid dynamics calculations of blood pressure gradients in the dural venous sinuses of patients with IIH. Pressure gradients are shown as a percentage of the blood pressure in the superior sagittal sinus (assigned as 100% in each patient). Patients without pathologic pressure gradients (*upper row*) show very little pressure drop across venous sinus stenoses compared with patients with pathologic pressure gradients (*lower row*). Sinuses are truncated at the posterior third of the superior sagittal sinus, midpoint of the straight sinus, and the end of each sigmoid sinus (see "Materials and Methods") and are shown in a right anterior oblique/Towne projection.

The average WSS gradient across stenotic segments (defined as the difference in WSS between the narrowest point of each stenosis and the midpoint of the ipsilateral sigmoid sinus) was 37.66 ± 48.39 Pa for the pathologic group and 7.02 ± 13.60 Pa for the nonpathologic group.

Figures 1 and 2 are visual depictions of blood pressure and WSS in the dural venous sinus models. Blood pressure is displayed as a percentage of the pressure in the superior sagittal sinus to normalize the results of pressure drops across the stenotic segments, while WSS is shown on a constant scale. This display permits comparison between patients with and without pathology. Visual inspection suggests minimal or low pressure drops across stenotic segments in the nonpathologic group (Fig 1, top row), compared with more substantial reduction in the pathologic group (Fig 1, lower row). Wall shear stress also appears minimally changed in the nonpathologic group (Fig 2, upper row) but elevated at and downstream of stenotic segments in the pathologic group (Fig 2, lower row).

Figure 3 shows 2D blood flow velocity profiles across dural venous sinus stenoses in patients in the nonpathologic (upper row) and pathologic groups (lower row). Projections are oriented through a cross-section of the maximal area of stenosis in each case. Visual inspection demonstrates substantially higher poststenotic velocities and disordered flow in the patients with pathology. The elevated velocities in Fig 3 correspond to the increased WSS and pressure drops in patients with pathology in Figs 1 and 2, while lower peak poststenotic velocities mirror the minimal WSS elevation and pressure drop seen in patients without pathology.
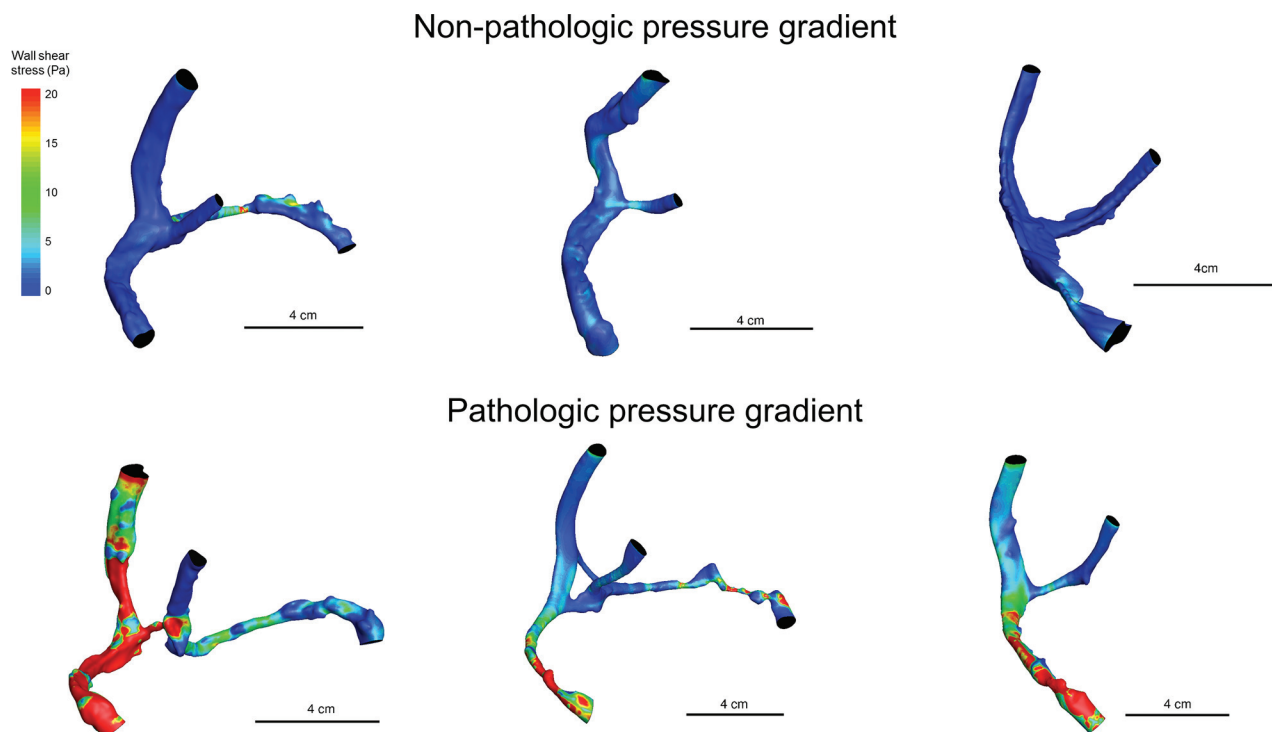
Non-pathologic pressure gradient

Pathologic pressure gradient

FIG 2. Computational fluid dynamics calculations of wall shear stress in the dural venous sinuses of patients with IIH. Patients without pathologic pressure gradients (*upper row*) show very little change in WSS at and beyond venous sinus stenoses compared with patients with pathologic pressure gradients (*lower row*), who have more severe elevations in WSS.
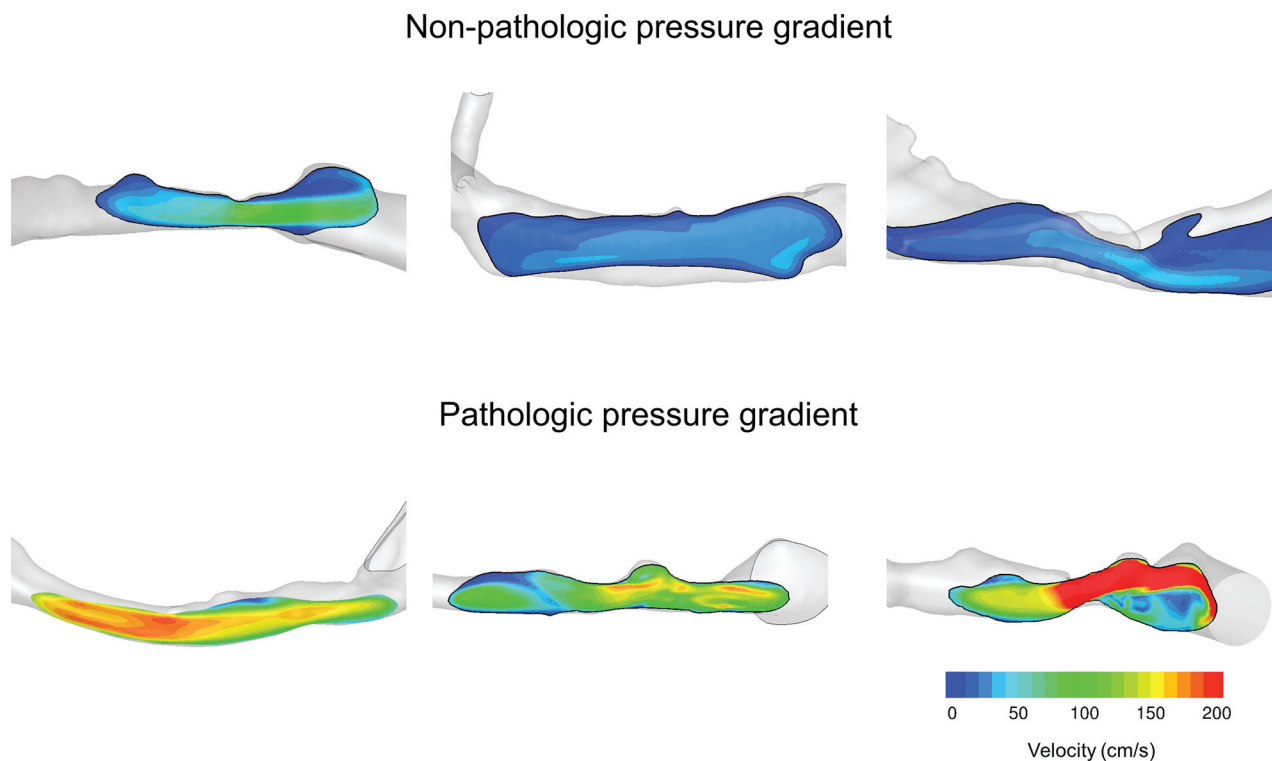
Non-pathologic pressure gradient

Pathologic pressure gradient

FIG 3. Computational fluid dynamics calculations of 2D velocity profiles oriented through the point of maximal venous sinus stenoses in patients in the nonpathologic (*upper row*) and pathologic (*lower row*) groups. Blood flow is from left to right. Substantially higher blood flow velocity is observed across stenoses in patients in the pathologic group.

The On-line Table shows CFD results without the virtual microcatheter. The effect of the virtual microcatheter on CFD was minimal on both total outflow (mean outflow reduction, 7.76% ± 3.98%) and WSS gradients across each transverse-sigmoid junction or stenosis (mean WSS reduction, 1.81% ± 24.19%).

DISCUSSION

We have modeled the hemodynamic environment of patients with IIH with dural venous sinus stenosis. Our CFD models used patient-specific anatomic information from each patient's MR venography and incorporated patient-specific venographic manometry measurements for use as boundary conditions. Patient-specific inlet and outlet boundary conditions have been shown to be more accurate than stereotypic boundary conditions (derived from literature averages of individual cases or healthy volunteer cohorts) in the CFD modeling of other cerebrovascular diseases such as intracranial aneurysms.[8,9] These CFD models permit the comparison of the hemodynamics of patients with IIH with similar anatomic venous sinus stenoses to better understand why some patients' stenoses were pathologic and were responsive to treatment with dural venous sinus stent placement, while others were not.

Patients with pathologic pressure gradients did have higher overall venous outflow rates through the transverse and sigmoid sinuses than those with low or absent pressure gradients (1041 versus 358 mL/min). The high flow rate in patient 4, who had a pathologic pressure gradient, may be an overestimate due to errors inherent in CFD reconstructions from MR venography data with large voxel sizes but is near previously published values of overall cerebral blood flow.[10] Despite anatomic abnormalities in both groups, flow rates of patients without pathology were similar to previously reported values for jugular flow in healthy controls.[11] This finding supports the theory that the presence of a stenotic or atretic segment may be necessary but not sufficient to cause pathologic pressure gradients across venous stenosis, because the presence of an atretic transverse/sigmoid sinus system (with 100% of outflow through the remaining stenotic segment) was seen in patients with and without pathologic pressure gradients in the current study, and others have observed no correlation between stenosis severity and IIH symptoms.[12] The presence of unilateral sinus hypoplasia or atresia in up to 33% of asymptomatic patients also argues against a purely anatomic source of flow disturbance.[13,14]

Wall shear stress also differed between patient groups. In the nonpathologic group, minimal or no elevation in WSS was observed in stenotic segments, while large elevations in WSS were seen at and downstream from stenoses in the pathologic group. Since WSS has been related to downstream vascular resistance,[15] the difference in WSS profiles between groups further underscores the lack of adequate collateral pathways (and thus increased vascular resistance across the stenosis) in the pathologic group. Similarly, the 2D velocity profiles across the stenosis in patients with and without pathology demonstrate higher poststenotic velocity in the pathologic group, indicating more disordered flow and vascular resistance, which could also correspond to reduced collaterals.

While the underlying mechanism for venous sinus stenosis in patients with IIH remains unclear, these results suggest that patients with anatomic but not pathologic stenosis may have collateral venous drainage in addition to the transverse/sigmoid sinus system. These collateral venous pathways prevent the increased resistance of an anatomic stenosis from affecting the overall pressure gradient across it and thus limit the elevation of blood pres-

sure upstream from the stenosis. In patients in whom collaterals are sparse or absent, the resistance created by the narrowing of 1 or both primary venous outflow channels (the sigmoid sinuses) increases the pressure upstream from the stenosis, creating a pathologic gradient and elevating the pressure in the entire venous sinus system. Cerebral venous hypertension further limits CSF reabsorption, increasing intracranial pressure and further exacerbating IIH by compressing the already stenosed segment acting as a Starling resistor.[16,17] On the other hand, in vitro and animal studies on the influence of extravascular pressure on cerebral venous outflow do not perfectly follow this model.[18]

Because the compliance and elasticity of the dural venous sinuses are not known, we are unable to incorporate intracranial pressure measurements into the model calculations. The near-instantaneous nature of the CFD calculations (by using a single time point of venous pressure) should limit the effects of intracranial pressure on our calculations, but the complex relationship between intracranial pressure and pathologic dural venous sinus stenosis remains incompletely explained.[18] In the pathologic group, all 3 patients had intracranial pressures of >40 cm H_2O, while in the nonpathologic group, intracranial pressures were lower (<30 cm H_2O). Future study of CFD before and after stent treatment would be improved with incorporation of intracranial pressure changes to ensure accurate modeling of the influence of external compression on the dural venous sinus stenosis.

The results of this study could have practical applications for the noninvasive screening of patients with IIH for a pathologic pressure gradient. A review of our large cohort of 158 patients with and without IIH who underwent diagnostic cerebral venography and manometry showed that noninvasive vascular imaging (such as MR venography and CT venography) was an imperfect predictor of the pathologic pressure gradient, even in the presence of anatomic dural venous sinus stenosis.[19] This finding is consistent with the findings of the current study of different flow and WSS profiles between patients with and without pathology, despite similar degrees of anatomic stenoses or atresia. Recent advances in noninvasive quantitative phase-contrast MR venography show promise in measuring blood flow through venous sinuses.[20] Applying such measurements as boundary conditions in the CFD simulation methodology of the current study may allow noninvasive, patient-specific, and accurate determination of pathologic and nonpathologic stenoses without the need for invasive venography. This method could be used for enhanced screening of patients with IIH at the time of diagnosis and is under investigation by our group. In addition, the hemodynamic changes before and after stent placement across pathologic segments could be virtually modeled before the procedure to help predict the restoration of normal blood pressure, blood flow, and WSS.

We observed a minimal effect on flow when the virtual microcatheter was placed across the venous sinus stenosis in our simulations. This is an important finding relative to the methods by which pressure gradients are obtained in venographic manometry because a catheter placed through an already narrow vessel (such as a venous sinus stenosis) could impart a "loading error," further reducing the cross-sectional area of the lumen and falsely elevating the pressure measurements.[21] This is a common critique of

the results of venographic manometry because there is concern that the procedure in which pressures are measured may skew the measured results and potentially affect patient treatment strategy. However, we observed a minimal loading error for both outflow and the WSS gradients, and the large SD observed for WSS gradients was the result of the effect of the microcatheter on very small ($<$1 Pa) absolute WSS values in 3 patients. This minimal loading error is unlikely to be clinically relevant because a substantially larger error would be required to create a falsely elevated flow leading to a pressure gradient of $\geq$8 mm Hg, which would change clinical decision-making toward stent placement.[5] Other CFD studies using patient-specific boundary conditions measured by intravascular devices may require integration of the presence of the device into determining the load error, though in our study, this did not have a substantial influence on calculations and should not be considered as a source of clinically relevant error on venographic manometry measurements in patients with IIH.

A simplified mathematic model was also created in an attempt to predict the degree of flow disturbance created by a microcatheter of a certain diameter (On-line Appendix). This model predicts that a microcatheter one-tenth of the diameter of the stenotic segment of the vessel causes approximately 40% reduction in flow, and that a microcatheter one-hundredth of the diameter of the stenosis causes approximately 22% reduction in flow assuming that the pressure gradient is fixed. The ability of the model to make quantitative predictions is limited by a number of important factors. In a stenosis, the spatial accelerations are likely important and the flow is not fully developed; thus, these features violate a key assumption of the model. More important, the excess resistance is highly dependent on the individual anatomy of each stenosis and not just the ratio of the diameters of the catheter and stenosis as the model predicts. Thus, CFD modeling with patient-specific anatomic and physiologic data as presented above is more likely to reflect accurate hemodynamic conditions on a case-by-case basis.

This work has several limitations. First, the sample size is small, precluding statistical comparison between patients with and without pathology. However, this study demonstrates the methodology for CFD modeling of the dural venous sinuses by using patient-specific physiologic measurements as boundary conditions, which has not been reported before, to our knowledge. Second, the voxel size of the MR venography used to reconstruct the dural venous sinuses, which ranged from 0.43 to 0.86 mm^3, could potentially miss fine webbing that could be better seen by using high-resolution techniques such as conebeam CT venography[22] or felt during microcatheterization during invasive venography. A 10% error in stenosis diameter estimation can change the flow rate by 40%, and it is unclear how equally the errors in the reconstructions affect patients with and without pathology. Third, prescribing only the pressures (without velocities) as the CFD boundary conditions may be more susceptible to random errors subject to the precision of the pressure transducer ($\pm$1 mm Hg), especially in cases in which the pressure gradients are small. The prescribed pressure gradients in CFD may have relative errors of up to 25%, and the calculated flow rates may subsequently have similar relative errors. However, the relative errors are likely much smaller in pathologic cases in which large pressure

gradients were measured and are thus unlikely to be clinically significant. Fourth, there were differences in the severity of stenoses in patients with pathologic and nonpathologic stenoses. However, all patients had documented IIH and some degree of venous sinus abnormality (stenosis, atresia, or both), which could cause outflow abnormalities and influence hemodynamics across the entire dural sinus system, as has been proposed by others.[23]

CONCLUSIONS

Dural venous sinus stenosis in patients with IIH can be computationally modeled by using patient-specific anatomic and physiologic data. Increased overall blood flow and WSS were found in patients with a pathologic pressure gradient.

REFERENCES

1. Higgins JN, Owler BK, Cousins C, et al. **Venous sinus stenting for refractory benign intracranial hypertension.** *Lancet* 2002;359: 228–30 Medline
2. Puffer RC, Mustafa W, Lanzino G. **Venous sinus stenting for idiopathic intracranial hypertension: a review of the literature.** *J Neurointerv Surg* 2013;5:483–86 CrossRef Medline
3. Farb RI, Vanek I, Scott JN, et al. **Idiopathic intracranial hypertension: the prevalence and morphology of sinovenous stenosis.** *Neurology* 2003;60:1418–24 CrossRef Medline
4. Albuquerque FC, Dashti SR, Hu YC, et al. **Intracranial venous sinus stenting for benign intracranial hypertension: clinical indications, technique, and preliminary results.** *World Neurosurg* 2011;75:648–52; discussion 592–95 CrossRef Medline
5. Ahmed RM, Wilkinson M, Parker GD, et al. **Transverse sinus stenting for idiopathic intracranial hypertension: a review of 52 patients and of model predictions.** *AJNR Am J Neuroradiol* 2011;32:1408–14 CrossRef Medline
6. Bateman GA. **Arterial inflow and venous outflow in idiopathic intracranial hypertension associated with venous outflow stenoses.** *J Clin Neurosci* 2008;15:402–08 CrossRef Medline
7. Friedman DI, Jacobson DM. **Diagnostic criteria for idiopathic intracranial hypertension.** *Neurology* 2002;59:1492–95 CrossRef Medline
8. McGah PM, Levitt MR, Barbour MC, et al. **Accuracy of computational cerebral aneurysm hemodynamics using patient-specific endovascular measurements.** *Ann Biomed Eng* 2014;42:503–14 CrossRef Medline
9. Venugopal P, Valentino D, Schmitt H, et al. **Sensitivity of patient-specific numerical simulation of cerebral aneurysm hemodynamics to inflow boundary conditions.** *J Neurosurg* 2007;106:1051–60 CrossRef Medline
10. Ford MD, Alperin N, Lee SH, et al. **Characterization of volumetric flow rate waveforms in the normal internal carotid and vertebral arteries.** *Physiol Meas* 2005;26:477–88 CrossRef Medline
11. Kim J, Thacker NA, Bromiley PA, et al. **Prediction of the jugular venous waveform using a model of CSF dynamics.** *AJNR Am J Neuroradiol* 2007;28:983–89 Medline
12. Riggeal BD, Bruce BB, Saindane AM, et al. **Clinical course of idiopathic intracranial hypertension with transverse sinus stenosis.** *Neurology* 2013;80:289–95 CrossRef Medline
13. Ayanzen RH, Bird CR, Keller PJ, et al. **Cerebral MR venography:**

normal anatomy and potential diagnostic pitfalls. *AJNR Am J Neuroradiol* 2000;21:74–78 Medline

14. Durst CR, Ornan DA, Reardon MA, et al. **Prevalence of dural venous sinus stenosis and hypoplasia in a generalized population.** *J Neurointerv Surg* 2016 Jan 8. [Epub ahead of print] CrossRef Medline

15. Van Steenkiste C, Trachet B, Casteleyn C, et al. **Vascular corrosion casting: analyzing wall shear stress in the portal vein and vascular abnormalities in portal hypertensive and cirrhotic rodents.** *Lab Invest* 2010;90:1558–72 CrossRef Medline

16. De Simone R, Ranieri A, Bonavita V. **Advancement in idiopathic intracranial hypertension pathogenesis: focus on sinus venous stenosis.** *Neurol Sci* 2010;31(suppl 1):S33–39 CrossRef Medline

17. Stevens SA, Previte M, Lakin WD, et al. **Idiopathic intracranial hypertension and transverse sinus stenosis: a modelling study.** *Math Med Biol* 2007;24:85–109 Medline

18. Schaller B. **Physiology of cerebral venous blood flow: from experimental data in animals to normal function in humans.** *Brain Res Brain Res Rev* 2004;46:243–60 CrossRef Medline

19. Levitt MR, Hlubek RJ, Moon K, et al. **Incidence and predictors of dural venous sinus pressure gradient in idiopathic intracranial hypertension and non-idiopathic intracranial hypertension headache patients: results from 164 cerebral venograms.** *J Neurosurg* 2016 Mar 11. [Epub ahead of print] Medline

20. Esfahani DR, Stevenson M, Moss HE, et al. **Quantitative magnetic resonance venography is correlated with intravenous pressures before and after venous sinus stenting: implications for treatment and monitoring.** *Neurosurgery* 2015;77:254–60 CrossRef Medline

21. Torii R, Wood NB, Hughes AD, et al. **A computational study on the influence of catheter-delivered intravascular probes on blood flow in a coronary artery model.** *J Biomech* 2007;40:2501–09 CrossRef Medline

22. Hiu T, Kitagawa N, Morikawa M, et al. **Efficacy of DynaCT digital angiography in the detection of the fistulous point of dural arteriovenous fistulas.** *AJNR Am J Neuroradiol* 2009;30:487–91 CrossRef Medline

23. Rohr A, Bindeballe J, Riedel C, et al. **The entire dural sinus tree is compressed in patients with idiopathic intracranial hypertension: a longitudinal, volumetric magnetic resonance imaging study.** *Neuroradiology* 2012;54:25–33 CrossRef Medline